

Search for Technicolor Particles Produced in Association with a W Boson at CDF

T. Aaltonen,²⁴ J. Adelman,¹⁴ B. Álvarez González^v,¹² S. Amerio^{dd},⁴⁴ D. Amidei,³⁵
 A. Anastassov,³⁹ A. Annovi,²⁰ J. Antos,¹⁵ G. Apollinari,¹⁸ A. Apresyan,⁴⁹ T. Arisawa,⁵⁸
 A. Artikov,¹⁶ J. Asaadi,⁵⁴ W. Ashmanskas,¹⁸ A. Attal,⁴ A. Aurisano,⁵⁴ F. Azfar,⁴³
 W. Badgett,¹⁸ A. Barbaro-Galtieri,²⁹ V.E. Barnes,⁴⁹ B.A. Barnett,²⁶ P. Barria^{ff},⁴⁷
 P. Bartos,¹⁵ G. Bauer,³³ P.-H. Beauchemin,³⁴ F. Bedeschi,⁴⁷ D. Beecher,³¹ S. Behari,²⁶
 G. Bellettini^{ee},⁴⁷ J. Bellinger,⁶⁰ D. Benjamin,¹⁷ A. Beretvas,¹⁸ A. Bhatti,⁵¹ M. Binkley,¹⁸
 D. Bisello^{dd},⁴⁴ I. Bizjak^{jj},³¹ R.E. Blair,² C. Blocker,⁷ B. Blumenfeld,²⁶ A. Bocci,¹⁷
 A. Bodek,⁵⁰ V. Boisvert,⁵⁰ D. Bortoletto,⁴⁹ J. Boudreau,⁴⁸ A. Boveia,¹¹ B. Brau^a,¹¹
 A. Bridgeman,²⁵ L. Brigliadori^{cc},⁶ C. Bromberg,³⁶ E. Brubaker,¹⁴ J. Budagov,¹⁶
 H.S. Budd,⁵⁰ S. Budd,²⁵ K. Burkett,¹⁸ G. Busetto^{dd},⁴⁴ P. Bussey,²² A. Buzatu,³⁴
 K. L. Byrum,² S. Cabrera^x,¹⁷ C. Calancha,³² S. Camarda,⁴ M. Campanelli,³¹
 M. Campbell,³⁵ F. Canelli¹⁴,¹⁸ A. Canepa,⁴⁶ B. Carls,²⁵ D. Carlsmith,⁶⁰ R. Carosi,⁴⁷
 S. Carrilloⁿ,¹⁹ S. Carron,¹⁸ B. Casal,¹² M. Casarsa,¹⁸ A. Castro^{cc},⁶ P. Catastini^{ff},⁴⁷
 D. Cauz,⁵⁵ V. Cavaliere^{ff},⁴⁷ M. Cavalli-Sforza,⁴ A. Cerri,²⁹ L. Cerrito^q,³¹ S.H. Chang,²⁸
 Y.C. Chen,¹ M. Chertok,⁸ G. Chiarelli,⁴⁷ G. Chlachidze,¹⁸ F. Chlebana,¹⁸ K. Cho,²⁸
 D. Chokheli,¹⁶ J.P. Chou,²³ K. Chung^o,¹⁸ W.H. Chung,⁶⁰ Y.S. Chung,⁵⁰ T. Chwalek,²⁷
 C.I. Ciobanu,⁴⁵ M.A. Ciocci^{ff},⁴⁷ A. Clark,²¹ D. Clark,⁷ G. Compostella,⁴⁴ M.E. Convery,¹⁸
 J. Conway,⁸ M. Corbo,⁴⁵ M. Cordelli,²⁰ C.A. Cox,⁸ D.J. Cox,⁸ F. Crescioli^{ee},⁴⁷
 C. Cuenca Almenar,⁶¹ J. Cuevas^v,¹² R. Culbertson,¹⁸ J.C. Cully,³⁵ D. Dagenhart,¹⁸
 M. Datta,¹⁸ T. Davies,²² P. de Barbaro,⁵⁰ S. De Cecco,⁵² A. Deisher,²⁹ G. De Lorenzo,⁴
 M. Dell'Orso^{ee},⁴⁷ C. Deluca,⁴ L. Demortier,⁵¹ J. Deng^f,¹⁷ M. Deninno,⁶ M. d'Errico^{dd},⁴⁴
 A. Di Canto^{ee},⁴⁷ G.P. di Giovanni,⁴⁵ B. Di Ruzza,⁴⁷ J.R. Dittmann,⁵ M. D'Onofrio,⁴
 S. Donati^{ee},⁴⁷ P. Dong,¹⁸ T. Dorigo,⁴⁴ S. Dube,⁵³ K. Ebina,⁵⁸ A. Elagin,⁵⁴
 R. Erbacher,⁸ D. Errede,²⁵ S. Errede,²⁵ N. Ershaidat^{bb},⁴⁵ R. Eusebi,⁵⁴ H.C. Fang,²⁹
 S. Farrington,⁴³ W.T. Fedorko,¹⁴ R.G. Feild,⁶¹ M. Feindt,²⁷ J.P. Fernandez,³²
 C. Ferrazza^{gg},⁴⁷ R. Field,¹⁹ G. Flanagan^s,⁴⁹ R. Forrest,⁸ M.J. Frank,⁵ M. Franklin,²³
 J.C. Freeman,¹⁸ I. Furic,¹⁹ M. Gallinaro,⁵¹ J. Galyardt,¹³ F. Garberson,¹¹ J.E. Garcia,²¹
 A.F. Garfinkel,⁴⁹ P. Garosi^{ff},⁴⁷ H. Gerberich,²⁵ D. Gerdes,³⁵ A. Gessler,²⁷ S. Giagu^{hh},⁵²

V. Giakoumopoulou,³ P. Giannetti,⁴⁷ K. Gibson,⁴⁸ J.L. Gimmell,⁵⁰ C.M. Ginsburg,¹⁸
N. Giokaris,³ M. Giordaniⁱⁱ,⁵⁵ P. Giromini,²⁰ M. Giunta,⁴⁷ G. Giurgiu,²⁶ V. Glagolev,¹⁶
D. Glenzinski,¹⁸ M. Gold,³⁸ N. Goldschmidt,¹⁹ A. Golossanov,¹⁸ G. Gomez,¹²
G. Gomez-Ceballos,³³ M. Goncharov,³³ O. González,³² I. Gorelov,³⁸ A.T. Goshaw,¹⁷
K. Goulianatos,⁵¹ A. Gresele^{dd},⁴⁴ S. Grinstein,⁴ C. Grosso-Pilcher,¹⁴ R.C. Group,¹⁸
U. Grundler,²⁵ J. Guimaraes da Costa,²³ Z. Gunay-Unalan,³⁶ C. Haber,²⁹ S.R. Hahn,¹⁸
E. Halkiadakis,⁵³ B.-Y. Han,⁵⁰ J.Y. Han,⁵⁰ F. Happacher,²⁰ K. Hara,⁵⁶ D. Hare,⁵³
M. Hare,⁵⁷ R.F. Harr,⁵⁹ M. Hartz,⁴⁸ K. Hatakeyama,⁵ C. Hays,⁴³ M. Heck,²⁷
J. Heinrich,⁴⁶ M. Herndon,⁶⁰ J. Heuser,²⁷ S. Hewamanage,⁵ D. Hidas,⁵³ C.S. Hill^c,¹¹
D. Hirschbuehl,²⁷ A. Hocker,¹⁸ S. Hou,¹ M. Houlden,³⁰ S.-C. Hsu,²⁹ R.E. Hughes,⁴⁰
M. Hurwitz,¹⁴ U. Husemann,⁶¹ M. Hussein,³⁶ J. Huston,³⁶ J. Incandela,¹¹ G. Introzzi,⁴⁷
M. Iori^{hh},⁵² A. Ivanov^p,⁸ E. James,¹⁸ D. Jang,¹³ B. Jayatilaka,¹⁷ E.J. Jeon,²⁸ M.K. Jha,⁶
S. Jindariani,¹⁸ W. Johnson,⁸ M. Jones,⁴⁹ K.K. Joo,²⁸ S.Y. Jun,¹³ J.E. Jung,²⁸ T.R. Junk,¹⁸
T. Kamon,⁵⁴ D. Kar,¹⁹ P.E. Karchin,⁵⁹ Y. Kato^m,⁴² R. Kephart,¹⁸ W. Ketchum,¹⁴
J. Keung,⁴⁶ V. Khotilovich,⁵⁴ B. Kilminster,¹⁸ D.H. Kim,²⁸ H.S. Kim,²⁸ H.W. Kim,²⁸
J.E. Kim,²⁸ M.J. Kim,²⁰ S.B. Kim,²⁸ S.H. Kim,⁵⁶ Y.K. Kim,¹⁴ N. Kimura,⁵⁸ L. Kirsch,⁷
S. Klimenko,¹⁹ K. Kondo,⁵⁸ D.J. Kong,²⁸ J. Konigsberg,¹⁹ A. Korytov,¹⁹ A.V. Kotwal,¹⁷
M. Kreps,²⁷ J. Kroll,⁴⁶ D. Krop,¹⁴ N. Krumnack,⁵ M. Kruse,¹⁷ V. Krutelyov,¹¹ T. Kuhr,²⁷
N.P. Kulkarni,⁵⁹ M. Kurata,⁵⁶ S. Kwang,¹⁴ A.T. Laasanen,⁴⁹ S. Lami,⁴⁷ S. Lammel,¹⁸
M. Lancaster,³¹ R.L. Lander,⁸ K. Lannon^u,⁴⁰ A. Lath,⁵³ G. Latino^{ff},⁴⁷ I. Lazzizzera^{dd},⁴⁴
T. LeCompte,² E. Lee,⁵⁴ H.S. Lee,¹⁴ J.S. Lee,²⁸ S.W. Lee^w,⁵⁴ S. Leone,⁴⁷ J.D. Lewis,¹⁸
C.-J. Lin,²⁹ J. Linacre,⁴³ M. Lindgren,¹⁸ E. Lipeles,⁴⁶ A. Lister,²¹ D.O. Litvintsev,¹⁸
C. Liu,⁴⁸ T. Liu,¹⁸ N.S. Lockyer,⁴⁶ A. Loginov,⁶¹ L. Lovas,¹⁵ D. Lucchesi^{dd},⁴⁴ J. Lueck,²⁷
P. Lujan,²⁹ P. Lukens,¹⁸ G. Lungu,⁵¹ J. Lys,²⁹ R. Lysak,¹⁵ D. MacQueen,³⁴ R. Madrak,¹⁸
K. Maeshima,¹⁸ K. Makhoul,³³ P. Maksimovic,²⁶ S. Malde,⁴³ S. Malik,³¹ G. Manca^e,³⁰
A. Manousakis-Katsikakis,³ F. Margaroli,⁴⁹ C. Marino,²⁷ C.P. Marino,²⁵ A. Martin,⁶¹
V. Martin^k,²² M. Martínez,⁴ R. Martínez-Ballarín,³² P. Mastrandrea,⁵² M. Mathis,²⁶
M.E. Mattson,⁵⁹ P. Mazzanti,⁶ K.S. McFarland,⁵⁰ P. McIntyre,⁵⁴ R. McNulty^j,³⁰
A. Mehta,³⁰ P. Mehtala,²⁴ A. Menzione,⁴⁷ C. Mesropian,⁵¹ T. Miao,¹⁸ D. Mietlicki,³⁵
N. Miladinovic,⁷ R. Miller,³⁶ C. Mills,²³ M. Milnik,²⁷ A. Mitra,¹ G. Mitselmakher,¹⁹

H. Miyake,⁵⁶ S. Moed,²³ N. Moggi,⁶ M.N. Mondragonⁿ,¹⁸ C.S. Moon,²⁸ R. Moore,¹⁸
 M.J. Morello,⁴⁷ J. Morlock,²⁷ P. Movilla Fernandez,¹⁸ J. Mülsenstädt,²⁹ A. Mukherjee,¹⁸
 Th. Muller,²⁷ P. Murat,¹⁸ M. Mussini^{cc},⁶ J. Nachtman^o,¹⁸ Y. Nagai,⁵⁶ J. Naganoma,⁵⁶
 K. Nakamura,⁵⁶ I. Nakano,⁴¹ A. Napier,⁵⁷ J. Nett,⁶⁰ C. Neu^z,⁴⁶ M.S. Neubauer,²⁵
 S. Neubauer,²⁷ J. Nielsen^g,²⁹ L. Nodulman,² M. Norman,¹⁰ O. Norniella,²⁵ E. Nurse,³¹
 L. Oakes,⁴³ S.H. Oh,¹⁷ Y.D. Oh,²⁸ I. Oksuzian,¹⁹ T. Okusawa,⁴² R. Orava,²⁴ K. Osterberg,²⁴
 S. Pagan Griso^{dd},⁴⁴ C. Pagliarone,⁵⁵ E. Palencia,¹⁸ V. Papadimitriou,¹⁸ A. Papaikonomou,²⁷
 A.A. Paramanov,² B. Parks,⁴⁰ S. Pashapour,³⁴ J. Patrick,¹⁸ G. Paulettaⁱⁱ,⁵⁵ M. Paulini,¹³
 C. Paus,³³ T. Peiffer,²⁷ D.E. Pellett,⁸ A. Penzo,⁵⁵ T.J. Phillips,¹⁷ G. Piacentino,⁴⁷
 E. Pianori,⁴⁶ L. Pinera,¹⁹ K. Pitts,²⁵ C. Plager,⁹ L. Pondrom,⁶⁰ K. Potamianos,⁴⁹
 O. Poukhov*,¹⁶ F. Prokoshin^y,¹⁶ A. Pronko,¹⁸ F. Ptahosⁱ,¹⁸ E. Pueschel,¹³ G. Punzi^{ee},⁴⁷
 J. Pursley,⁶⁰ J. Rademacker^c,⁴³ A. Rahaman,⁴⁸ V. Ramakrishnan,⁶⁰ N. Ranjan,⁴⁹
 I. Redondo,³² P. Renton,⁴³ M. Renz,²⁷ M. Rescigno,⁵² S. Richter,²⁷ F. Rimondi^{cc},⁶
 L. Ristori,⁴⁷ A. Robson,²² T. Rodrigo,¹² T. Rodriguez,⁴⁶ E. Rogers,²⁵ S. Rolli,⁵⁷ R. Roser,¹⁸
 M. Rossi,⁵⁵ R. Rossin,¹¹ P. Roy,³⁴ A. Ruiz,¹² J. Russ,¹³ V. Rusu,¹⁸ B. Rutherford,¹⁸
 H. Saarikko,²⁴ A. Safonov,⁵⁴ W.K. Sakumoto,⁵⁰ L. Santiⁱⁱ,⁵⁵ L. Sartori,⁴⁷ K. Sato,⁵⁶
 A. Savoy-Navarro,⁴⁵ P. Schlabach,¹⁸ A. Schmidt,²⁷ E.E. Schmidt,¹⁸ M.A. Schmidt,¹⁴
 M.P. Schmidt*,⁶¹ M. Schmitt,³⁹ T. Schwarz,⁸ L. Scodellaro,¹² A. Scribano^{ff},⁴⁷ F. Scuri,⁴⁷
 A. Sedov,⁴⁹ S. Seidel,³⁸ Y. Seiya,⁴² A. Semenov,¹⁶ L. Sexton-Kennedy,¹⁸ F. Sforza^{ee},⁴⁷
 A. Sfyrla,²⁵ S.Z. Shalhout,⁵⁹ T. Shears,³⁰ P.F. Shepard,⁴⁸ M. Shimojima^t,⁵⁶ S. Shiraishi,¹⁴
 M. Shochet,¹⁴ Y. Shon,⁶⁰ I. Shreyber,³⁷ A. Simonenko,¹⁶ P. Sinervo,³⁴ A. Sisakyan,¹⁶
 A.J. Slaughter,¹⁸ J. Slaunwhite,⁴⁰ K. Sliwa,⁵⁷ J.R. Smith,⁸ F.D. Snider,¹⁸ R. Snihur,³⁴
 A. Soha,¹⁸ S. Somalwar,⁵³ V. Sorin,⁴ P. Squillacioti^{ff},⁴⁷ M. Stanitzki,⁶¹ R. St. Denis,²²
 B. Stelzer,³⁴ O. Stelzer-Chilton,³⁴ D. Stentz,³⁹ J. Strologas,³⁸ G.L. Strycker,³⁵ J.S. Suh,²⁸
 A. Sukhanov,¹⁹ I. Suslov,¹⁶ A. Taffard^f,²⁵ R. Takashima,⁴¹ Y. Takeuchi,⁵⁶ R. Tanaka,⁴¹
 J. Tang,¹⁴ M. Tecchio,³⁵ P.K. Teng,¹ J. Thom^h,¹⁸ J. Thome,¹³ G.A. Thompson,²⁵
 E. Thomson,⁴⁶ P. Tipton,⁶¹ P. Ttito-Guzmán,³² S. Tkaczyk,¹⁸ D. Toback,⁵⁴ S. Tokar,¹⁵
 K. Tollefson,³⁶ T. Tomura,⁵⁶ D. Tonelli,¹⁸ S. Torre,²⁰ D. Torretta,¹⁸ P. Totaroⁱⁱ,⁵⁵
 S. Tourneur,⁴⁵ M. Trovato^{gg},⁴⁷ S.-Y. Tsai,¹ Y. Tu,⁴⁶ N. Turini^{ff},⁴⁷ F. Ukegawa,⁵⁶

* Deceased

S. Uozumi,²⁸ N. van Remortel^b,²⁴ A. Varganov,³⁵ E. Vataga^{gg},⁴⁷ F. Vázquezⁿ,¹⁹ G. Velev,¹⁸
 C. Vellidis,³ M. Vidal,³² I. Vila,¹² R. Vilar,¹² M. Vogel,³⁸ I. Volobouev^w,²⁹ G. Volpi^{ee},⁴⁷
 P. Wagner,⁴⁶ R.G. Wagner,² R.L. Wagner,¹⁸ W. Wagner^{aa},²⁷ J. Wagner-Kuhr,²⁷
 T. Wakisaka,⁴² R. Wallny,⁹ S.M. Wang,¹ A. Warburton,³⁴ D. Waters,³¹ M. Weinberger,⁵⁴
 J. Weinelt,²⁷ W.C. Wester III,¹⁸ B. Whitehouse,⁵⁷ D. Whiteson^f,⁴⁶ A.B. Wicklund,²
 E. Wicklund,¹⁸ S. Wilbur,¹⁴ G. Williams,³⁴ H.H. Williams,⁴⁶ P. Wilson,¹⁸ B.L. Winer,⁴⁰
 P. Wittich^h,¹⁸ S. Wolbers,¹⁸ C. Wolfe,¹⁴ H. Wolfe,⁴⁰ T. Wright,³⁵ X. Wu,²¹ F. Würthwein,¹⁰
 A. Yagil,¹⁰ K. Yamamoto,⁴² J. Yamaoka,¹⁷ U.K. Yang^r,¹⁴ Y.C. Yang,²⁸ W.M. Yao,²⁹
 G.P. Yeh,¹⁸ K. Yi^o,¹⁸ J. Yoh,¹⁸ K. Yorita,⁵⁸ T. Yoshida^l,⁴² G.B. Yu,¹⁷ I. Yu,²⁸ S.S. Yu,¹⁸
 J.C. Yun,¹⁸ A. Zanetti,⁵⁵ Y. Zeng,¹⁷ X. Zhang,²⁵ Y. Zheng^d,⁹ and S. Zucchelli^{cc}⁶

(CDF Collaboration[†])

¹*Institute of Physics, Academia Sinica,
Taipei, Taiwan 11529, Republic of China*

²*Argonne National Laboratory, Argonne, Illinois 60439*

³*University of Athens, 157 71 Athens, Greece*

⁴*Institut de Fisica d'Altes Energies,
Universitat Autònoma de Barcelona,
E-08193, Bellaterra (Barcelona), Spain*

[†] With visitors from ^aUniversity of Massachusetts Amherst, Amherst, Massachusetts 01003, ^bUniversiteit Antwerpen, B-2610 Antwerp, Belgium, ^cUniversity of Bristol, Bristol BS8 1TL, United Kingdom, ^dChinese Academy of Sciences, Beijing 100864, China, ^eIstituto Nazionale di Fisica Nucleare, Sezione di Cagliari, 09042 Monserrato (Cagliari), Italy, ^fUniversity of California Irvine, Irvine, CA 92697, ^gUniversity of California Santa Cruz, Santa Cruz, CA 95064, ^hCornell University, Ithaca, NY 14853, ⁱUniversity of Cyprus, Nicosia CY-1678, Cyprus, ^jUniversity College Dublin, Dublin 4, Ireland, ^kUniversity of Edinburgh, Edinburgh EH9 3JZ, United Kingdom, ^lUniversity of Fukui, Fukui City, Fukui Prefecture, Japan 910-0017 ^mKinki University, Higashi-Osaka City, Japan 577-8502 ⁿUniversidad Iberoamericana, Mexico D.F., Mexico, ^oUniversity of Iowa, Iowa City, IA 52242, ^pKansas State University, Manhattan, KS 66506 ^qQueen Mary, University of London, London, E1 4NS, England, ^rUniversity of Manchester, Manchester M13 9PL, England, ^sMuons, Inc., Batavia, IL 60510, ^tNagasaki Institute of Applied Science, Nagasaki, Japan, ^uUniversity of Notre Dame, Notre Dame, IN 46556, ^vUniversity de Oviedo, E-33007 Oviedo, Spain, ^wTexas Tech University, Lubbock, TX 79609, ^xIFIC(CSIC-Universitat de Valencia), 56071 Valencia, Spain, ^yUniversidad Tecnica Federico Santa Maria, 110v Valparaiso, Chile, ^zUniversity of Virginia, Charlottesville, VA 22906 ^{aa}Bergische Universität Wuppertal, 42097 Wuppertal, Germany, ^{bb}Yarmouk University, Irbid 211-63, Jordan ^{jj}On leave from J. Stefan Institute, Ljubljana, Slovenia,

⁵*Baylor University, Waco, Texas 76798*

⁶*Istituto Nazionale di Fisica Nucleare Bologna,*

^{cc}*University of Bologna, I-40127 Bologna, Italy*

⁷*Brandeis University, Waltham, Massachusetts 02254*

⁸*University of California, Davis, Davis, California 95616*

⁹*University of California, Los Angeles, Los Angeles, California 90024*

¹⁰*University of California, San Diego, La Jolla, California 92093*

¹¹*University of California, Santa Barbara, Santa Barbara, California 93106*

¹²*Instituto de Fisica de Cantabria, CSIC-University of Cantabria, 39005 Santander, Spain*

¹³*Carnegie Mellon University, Pittsburgh, PA 15213*

¹⁴*Enrico Fermi Institute, University of Chicago, Chicago, Illinois 60637*

¹⁵*Comenius University, 842 48 Bratislava,*

Slovakia; Institute of Experimental Physics, 040 01 Kosice, Slovakia

¹⁶*Joint Institute for Nuclear Research, RU-141980 Dubna, Russia*

¹⁷*Duke University, Durham, North Carolina 27708*

¹⁸*Fermi National Accelerator Laboratory, Batavia, Illinois 60510*

¹⁹*University of Florida, Gainesville, Florida 32611*

²⁰*Laboratori Nazionali di Frascati, Istituto Nazionale*

di Fisica Nucleare, I-00044 Frascati, Italy

²¹*University of Geneva, CH-1211 Geneva 4, Switzerland*

²²*Glasgow University, Glasgow G12 8QQ, United Kingdom*

²³*Harvard University, Cambridge, Massachusetts 02138*

²⁴*Division of High Energy Physics, Department of Physics,
University of Helsinki and Helsinki Institute of Physics, FIN-00014, Helsinki, Finland*

²⁵*University of Illinois, Urbana, Illinois 61801*

²⁶*The Johns Hopkins University, Baltimore, Maryland 21218*

²⁷*Institut für Experimentelle Kernphysik,*

Karlsruhe Institute of Technology, D-76131 Karlsruhe, Germany

²⁸*Center for High Energy Physics: Kyungpook National University,
Daegu 702-701, Korea; Seoul National University, Seoul 151-742,
Korea; Sungkyunkwan University, Suwon 440-746,*

Korea; Korea Institute of Science and Technology Information,

*Daejeon 305-806, Korea; Chonnam National University, Gwangju 500-757,
Korea; Chonbuk National University, Jeonju 561-756, Korea*

²⁹Ernest Orlando Lawrence Berkeley National Laboratory, Berkeley, California 94720

³⁰University of Liverpool, Liverpool L69 7ZE, United Kingdom

³¹University College London, London WC1E 6BT, United Kingdom

³²Centro de Investigaciones Energeticas

Medioambientales y Tecnologicas, E-28040 Madrid, Spain

³³Massachusetts Institute of Technology, Cambridge, Massachusetts 02139

*³⁴Institute of Particle Physics: McGill University, Montréal,
Québec, Canada H3A 2T8; Simon Fraser University, Burnaby,
British Columbia, Canada V5A 1S6; University of Toronto,
Toronto, Ontario, Canada M5S 1A7; and TRIUMF,
Vancouver, British Columbia, Canada V6T 2A3*

³⁵University of Michigan, Ann Arbor, Michigan 48109

³⁶Michigan State University, East Lansing, Michigan 48824

³⁷Institution for Theoretical and Experimental Physics, ITEP, Moscow 117259, Russia

³⁸University of New Mexico, Albuquerque, New Mexico 87131

³⁹Northwestern University, Evanston, Illinois 60208

⁴⁰The Ohio State University, Columbus, Ohio 43210

⁴¹Okayama University, Okayama 700-8530, Japan

⁴²Osaka City University, Osaka 588, Japan

⁴³University of Oxford, Oxford OX1 3RH, United Kingdom

⁴⁴Istituto Nazionale di Fisica Nucleare, Sezione di Padova-Trento,

^{dd}University of Padova, I-35131 Padova, Italy

⁴⁵LPNHE, Universite Pierre et Marie

Curie/IN2P3-CNRS, UMR7585, Paris, F-75252 France

⁴⁶University of Pennsylvania, Philadelphia, Pennsylvania 19104

⁴⁷Istituto Nazionale di Fisica Nucleare Pisa, ^{ee}University of Pisa,

^{ff}University of Siena and ^{gg}Scuola Normale Superiore, I-56127 Pisa, Italy

⁴⁸University of Pittsburgh, Pittsburgh, Pennsylvania 15260

⁴⁹Purdue University, West Lafayette, Indiana 47907

⁵⁰University of Rochester, Rochester, New York 14627

⁵¹*The Rockefeller University, New York, New York 10021*

⁵²*Istituto Nazionale di Fisica Nucleare, Sezione di Roma 1,*

^{hh}*Sapienza Università di Roma, I-00185 Roma, Italy*

⁵³*Rutgers University, Piscataway, New Jersey 08855*

⁵⁴*Texas A&M University, College Station, Texas 77843*

⁵⁵*Istituto Nazionale di Fisica Nucleare Trieste/Udine,
I-34100 Trieste, ⁱⁱUniversity of Trieste/Udine, I-33100 Udine, Italy*

⁵⁶*University of Tsukuba, Tsukuba, Ibaraki 305, Japan*

⁵⁷*Tufts University, Medford, Massachusetts 02155*

⁵⁸*Waseda University, Tokyo 169, Japan*

⁵⁹*Wayne State University, Detroit, Michigan 48201*

⁶⁰*University of Wisconsin, Madison, Wisconsin 53706*

⁶¹*Yale University, New Haven, Connecticut 06520*

(Dated: December 3, 2009)

Abstract

We present a search for the technicolor particles ρ_T and π_T in the process $p\bar{p} \rightarrow \rho_T \rightarrow W\pi_T$ at a center of mass energy of $\sqrt{s} = 1.96$ TeV. The search uses a data sample corresponding to approximately 1.9 fb^{-1} of integrated luminosity accumulated by the CDF II detector at the Fermilab Tevatron. The event signature we consider is $W \rightarrow \ell\nu$ and $\pi_T \rightarrow b\bar{b}, b\bar{c}$ or $b\bar{u}$ depending on the π_T charge. We select events with a single high- p_T electron or muon, large missing transverse energy, and two jets. Jets corresponding to bottom quarks are identified with multiple b -tagging algorithms. The observed number of events and the invariant mass distributions are consistent with the standard model background expectations, and we exclude a region at 95% confidence level in the ρ_T - π_T mass plane. As a result, a large fraction of the region $m(\rho_T) = 180 - 250 \text{ GeV}/c^2$ and $m(\pi_T) = 95 - 145 \text{ GeV}/c^2$ is excluded.

PACS numbers: 13.85.Rm, 14.80.Bn

The mechanism of electroweak symmetry breaking in nature is still unknown. The standard model (SM) assumes the Higgs mechanism [1] but provides no explanation as to why there should be a fundamental scalar Higgs field with a non-zero vacuum expectation value. An alternative approach is to seek a dynamical mechanism for the symmetry breaking. The scenario known as technicolor [2–4] proposes a new strong interaction, modeled on QCD, which spontaneously breaks electroweak symmetry in an analogous way to the breaking of chiral symmetry in QCD. The strong technicolor interaction between the new technifermions results in a vacuum technifermion condensate which can break electroweak symmetry and hence give mass to the W^\pm and Z gauge bosons. As in QCD, the technicolor interaction should give rise to technipions (π_T) and other technimesons. In this Letter we report the results of a search for technipions produced in association with a W boson from technirho (ρ_T) decay, $\rho_T \rightarrow W\pi_T$, in the context of the technicolor straw man (TCSM) model [5]. Technirhos can be produced from an off-shell W or Z . Like the SM Higgs, the technipion coupling to fermions is proportional to mass, and hence the technipion predominantly decays to $b\bar{b}$, $b\bar{c}$, or $b\bar{u}$, depending on its charge. The resulting final state is identified by selecting events with exactly one high- p_T electron or muon candidate, large missing transverse energy, and two jets, at least one of which is identified as containing a b -quark (b -tagged).

Previous searches by the CDF and D0 experiments [6, 7] were limited not only by smaller data samples, but also by contamination from jets associated with charm or light-flavor quarks which can be falsely tagged as b -jets. The data sample used here corresponds to $1.9 \pm 0.1 \text{ fb}^{-1}$ of integrated luminosity, nearly five times the sample used in the previous Tevatron searches. To improve the purity of the selected event sample, the search described in this Letter employs the same b -tagging strategies that are used in the SM Higgs search in the $W + 2$ jets channel [8]. Previous searches for technicolor particles at LEP were able to exclude ρ_T production at 95% confidence level for $90 < m_{\rho_T} < 206.7 \text{ GeV}/c^2$, independently of the assumed π_T mass and other model parameters [9].

The CDF II [10] is a general purpose detector to study $p\bar{p}$ collisions at $\sqrt{s} = 1.96 \text{ TeV}$ at the Fermilab Tevatron. It consists of a cylindrical magnetic spectrometer, surrounded by electromagnetic and hadronic calorimeters. Charged particle tracking is performed with microstrip silicon detectors surrounded by a large cylindrical multilayer drift chamber, both immersed in a 1.4 T solenoidal magnetic field aligned coaxially with the incoming beams. Jets are identified as collections of electromagnetic and hadronic energy deposits

in calorimeter towers, which are clustered using an iterative cone algorithm with a cone of $\Delta R = \sqrt{(\Delta\phi)^2 + (\Delta\eta)^2} = 0.4$ [11]. Muons are identified by a system of drift chambers and scintillators placed outside the calorimeter at a depth of at least five nuclear interaction lengths from the interaction region.

Events are collected using high- p_T electron or muon triggers with a three-level selection filter. The first two levels identify purely electromagnetic calorimeter clusters, or require that track segments in the muon chambers align with tracks in the drift chamber having $p_T > 8 \text{ GeV}/c$. The third-level trigger requires an electron (muon) with $E_T > 18 \text{ GeV}$ ($p_T > 18 \text{ GeV}/c$).

Events are required to have exactly one electron or muon candidate, large missing transverse energy ($\cancel{E}_T > 20 \text{ GeV}$) [11], and two jets. The electron or muon must be within the central part of the detector, in the pseudorapidity regions $|\eta| < 1.1$ or $|\eta| < 1.0$, respectively, and must have $E_T > 20 \text{ GeV}$ or $p_T > 20 \text{ GeV}$. Because the lepton from a leptonic W decay is well isolated from the rest of the event, the cone of $\Delta R = 0.4$ surrounding the lepton is required to contain less than 10% of the lepton transverse energy. It must also be no more than 5 cm in z away from the primary event vertex, which is defined by fitting a subset of charged particle tracks in the event to a single vertex. To reduce the background from Z boson decays, we reject not only events with multiple high- p_T leptons, but also events in which the lepton and another high- p_T track of opposite sign form an invariant mass between $76 < M_{ll} < 106 \text{ GeV}/c^2$. Jets used in the analysis must fall within the acceptance of the silicon detector ($|\eta| < 2.0$) for reliable b -tagging, and they must have transverse energy greater than 20 GeV.

The primary background to this technicolor search is SM $W + 2$ jets production. However this process is dominated by light-flavor jets, while the technipion decay process should contain at least one b quark. Identifying these b -quark jets therefore helps to significantly suppress the background. We use two b -tagging algorithms: a secondary vertex finding algorithm [12] (SECVTX) and a jet probability tagging algorithm [13] (JETPROB). To further improve the purity of the SECVTX sample, a neural network (NN) filter has been trained to reject tagged jets originating from charm or light-quarks [12]. The selection cuts on the NN output are chosen to give 90% efficiency for true b -jets identified with SECVTX while rejecting $65 \pm 5\%$ for light-flavor jets and $50 \pm 5\%$ for charm jets, as measured using simulated events and verified with multijet data. The search sensitivity is maximized by using three

exclusive b -tagged event categories. The first category (ST+ST) contains events with two SECVTX b -tagged jets. The second category (ST+JP) consists of events where only one of the jets is b -tagged by SECVTX and the second jet is only b -tagged by JETPROB. The third category (ST+NNtag) is for events which do not belong to the first two categories but contain exactly one SECVTX b -tagged jet that also passes the NN filter. Because events with charm and light-flavor jets are unlikely to be double-tagged, the extra NN filter is not applied to double-tagged events.

The selected event sample includes contributions from other standard model processes. The largest backgrounds are due to $W +$ jets production, $t\bar{t}$ production, and non- W multijet production, with small contributions from single top, diboson (WW , WZ , ZZ), and $Z \rightarrow \tau\tau$ production. These backgrounds are estimated using the same methods as the standard model Higgs boson search analysis in the $W + 2$ jets channel [12]. A summary of the estimated backgrounds to the $W + 2$ jets final state that are described below is shown in Table I, along with the number of observed events in data and the expected technicolor signal events with $m_{\rho_T} = 200 \text{ GeV}/c^2$ and $m_{\pi_T} = 115 \text{ GeV}/c^2$.

The $W +$ jets contribution includes jets from b and c quarks, and light-flavor jets mistagged by the b -tagging algorithm. The effect of true $W +$ heavy-flavor production is estimated from a combination of data and simulation. We use the ALPGEN Monte Carlo program [14] to calculate the rate of $Wb\bar{b}$, $Wc\bar{c}$, and Wc production relative to inclusive $W +$ jets production. This relative rate is then applied to the observed $W +$ jets sample, after non- W and $t\bar{t}$ contributions have been subtracted. Finally, we apply b -tagging efficiencies and the NN filter rate calculated using the ALPGEN event samples.

Contributions from events with falsely tagged light-flavor jets (mistags) are estimated by measuring a mistag rate in inclusive jet data. The mistag rate is further modified by the NN filter efficiency. The resulting overall mistag rate is applied to the observed $W +$ jets sample to yield the number of mistagged events expected in the sample.

Events from $t\bar{t}$ production followed by leptonic W decay typically have two b jets from top decay, significant missing transverse energy, and one high- p_T lepton with additional jets if one of the W bosons from the top quarks decay hadronically. The $t\bar{t}$ contribution to the $\ell\nu b\bar{b}$ final state is estimated using simulated PYTHIA events [15]. It is normalized to the next-to-leading-order (NLO) cross section $\sigma_{t\bar{t}} = 6.7^{+0.7}_{-0.9} \text{ pb}$ calculated for $m_t = 175 \text{ GeV}/c^2$ [16]. The small contribution from production of single top quarks is estimated using MADEVENT [17]

and PYTHIA normalized to the NLO cross section [18].

The signature of W decay can also be mimicked by non- W multijet events which may contain a high- p_T reconstructed lepton and missing transverse energy. These can arise from semileptonic heavy-flavor decay or from hadrons misidentified as leptons. The reconstructed leptons from such events are rarely isolated from other energetic particles, as required by our event selection, and seldom yield large missing transverse energy. We therefore calculate the number of non- W events in our selected sample by extrapolating from sideband regions (defined in the space of lepton energy isolation and missing transverse energy) into the signal region [19].

Small contributions from diboson backgrounds (WW , WZ , and ZZ) are estimated using the NLO theoretical cross section calculations [20] and $Z \rightarrow \tau\tau$ backgrounds are estimated using the CDF result [21], with acceptances calculated using fully simulated events from the PYTHIA Monte Carlo program.

The dominant systematic uncertainty in the $W +$ heavy-flavor background is the correction factor for simulation derived from multijet data [19]. Different simulation inputs give different factors, and we find a 30% relative uncertainty on the background from heavy-flavor. The background from mistags has uncertainties on the rate correction due to particle interactions in detector material and on the NN rejection factor. Both are estimated to be 15% relative errors. Cross-checks of sideband data yield a 17% relative uncertainty on the non- W multijet estimate. The electroweak background estimates for diboson and single top are subject to uncertainties in the b -tagging efficiency and the cross section predictions.

The signal process in $\rho_T \rightarrow W\pi_T \rightarrow l\nu j_1 j_2$ is expected to show resonant peaks in both the dijet and $W + 2$ jets mass spectra. We reconstruct the p_z of the neutrino by constraining the invariant mass of the lepton-neutrino pair to the W boson mass, which gives a two-fold ambiguity. We select the solution with the smaller $|p_z|$, since that is more probable given the production mechanism of this heavy state; if there is no real solution, we set the imaginary part of solution to zero. Figure 1 shows the observed dijet mass spectra in the double tagged (ST+ST and ST+JP) and one SECVTX with NN filter tagged 2 jets samples, along with the distributions expected from the background processes. Figure 2 shows the Q -value distribution in each b -tagging category, the mass difference defined as $Q = m(\rho_T) - m(\pi_T) - m(W)$, which exploits the fact that the Q -value for the ρ_T decay is quite small and consequently the resolution of the mass difference is better than the mass

Selection	ST+ST	ST+JP	ST+NNtag
$Wb\bar{b}$	37.9 ± 16.9	31.2 ± 14.0	215.6 ± 92.3
$Wc\bar{c}$	2.9 ± 1.2	7.9 ± 3.4	167.0 ± 62.1
Mistag	3.9 ± 0.4	11.7 ± 0.9	107.1 ± 9.4
$t\bar{t}$	19.0 ± 2.9	15.6 ± 2.4	60.7 ± 9.3
Single top	8.5 ± 1.2	7.0 ± 1.0	44.0 ± 6.4
non-W	5.5 ± 1.0	9.6 ± 1.7	184.7 ± 33.0
WW	0.17 ± 0.02	0.9 ± 0.1	15.4 ± 1.9
WZ	2.41 ± 0.26	1.8 ± 0.2	7.6 ± 0.8
ZZ	0.06 ± 0.01	0.08 ± 0.01	0.31 ± 0.03
$Z \rightarrow \tau\tau$	0.25 ± 0.04	1.3 ± 0.2	7.3 ± 1.1
Total Bkg.	80.6 ± 18.8	87.0 ± 18.0	809.6 ± 159.4
$m(\rho_T^\pm, \pi_T^0) = (200, 115) \text{ GeV}/c^2$	11.2 ± 1.4	7.7 ± 1.1	20.7 ± 1.7
$m(\rho_T^0, \pi_T^\mp) = (200, 115) \text{ GeV}/c^2$	1.5 ± 0.3	2.8 ± 0.6	23.0 ± 2.0
Observed Events	83	90	805

TABLE I: Predicted sample composition and observed number of $W + 2$ jets in each b -tagging category, along with the expected signal events for a mass hypothesis of $m_{\rho_T} = 200 \text{ GeV}/c^2$ and $m_{\pi_T} = 115 \text{ GeV}/c^2$.

of the ρ_T itself. The signal distributions from the charged and neutral technicolor particles with $m_{\rho_T} = 200 \text{ GeV}/c^2$ and $m_{\pi_T} = 115 \text{ GeV}/c^2$ are also shown for comparison. There is no significant excess observed in either the dijet mass or Q -value distributions.

The acceptance for $\rho_T \rightarrow W\pi_T \rightarrow \ell\nu b\bar{b}, b\bar{c}, b\bar{u}$, including leptonic τ decays, is calculated from samples generated with the PYTHIA Monte Carlo program using ρ_T mass values between 180 and $250 \text{ GeV}/c^2$ with a step of $10 \text{ GeV}/c^2$. We set the parameters in the TCSM as: $N_{TC} = 4$, $M_V = M_A = 200 \text{ GeV}/c^2$, $Q_U = Q_D + 1$ and $\sin \chi = 1/3$, where N_{TC} is the number of technicolors, M_V is the vector technimeson decay parameter, M_A is the axial mass parameter for technivector decays to technipion, $Q_U(Q_D)$ is the charge of the up-type (down-type) technifermion, and $\sin \chi$ is the mixing angle between isotriplet technipion interaction and mass eigenstates. For this study, we consider the lightest technihadron

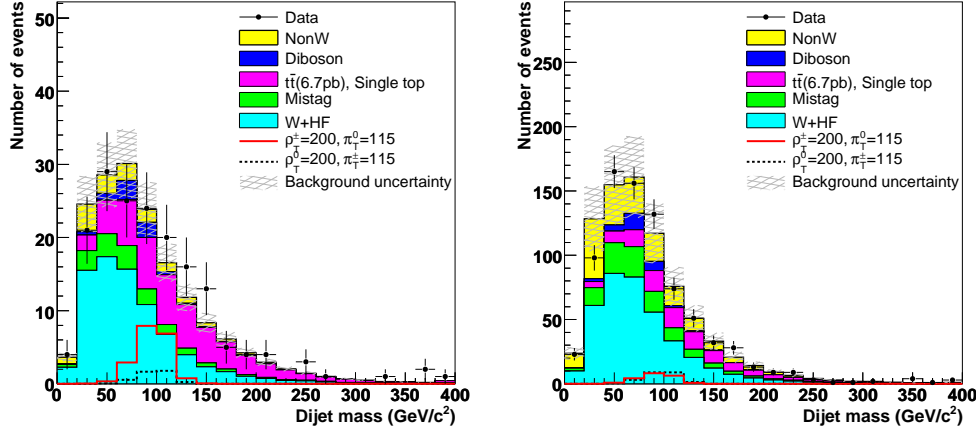


FIG. 1: Reconstructed dijet mass distributions for $W + 2$ jets events. The left is for double tags (ST+ST and ST+JP) and the right is for single tag (ST+NNtag) events.

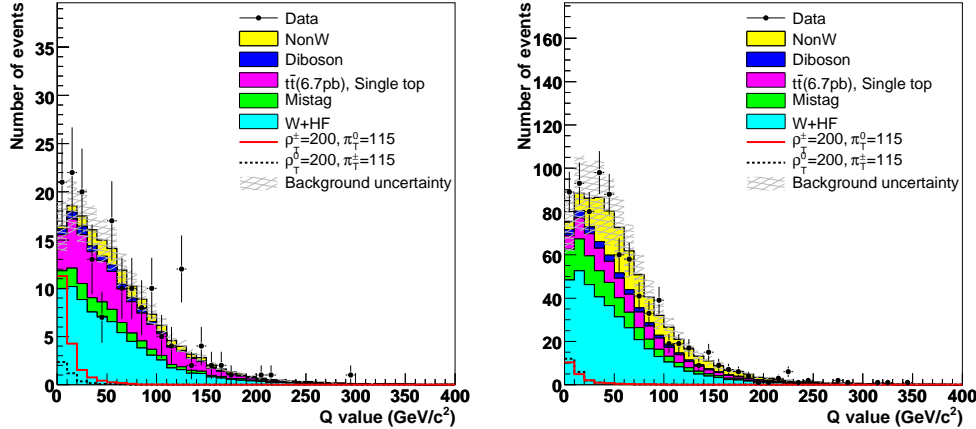


FIG. 2: Reconstructed Q -value distributions for $W + 2$ jets events, where $Q = m(\rho_T) - m(\pi_T) - m(W)$. The left is for double tags (ST+ST and ST+JP) and the right is for single tag (ST+NNtag) events.

masses in the $\rho_T - \pi_T$ mass plane $180 < m(\rho_T) < 250$ GeV/c 2 and $\max(m(\rho_T)/2, m(W)) < m(\pi_T) < m(\rho_T) - m(W)$ where the decay $\rho_T \rightarrow W\pi_T$ dominates. The cut-off $m(\rho_T)$ at 250 GeV/c 2 is set by the search sensitivity.

The total acceptances for ST+ST, ST+JP and ST+NNtag events of $\pi_T^0 \rightarrow b\bar{b}$ ($\pi_T^\pm \rightarrow b\bar{c}, b\bar{u}$) are $0.40 \pm 0.05\%$ ($0.05 \pm 0.01\%$), $0.27 \pm 0.04\%$ ($0.10 \pm 0.02\%$), and $0.73 \pm 0.06\%$ ($0.81 \pm 0.04\%$).

0.07%), respectively, for $m_{\rho_T} = 200 \text{ GeV}/c^2$ and $m_{\pi_T} = 115 \text{ GeV}/c^2$. The dominant systematic uncertainty on the acceptance for the $\pi_T^0 \rightarrow b\bar{b}$ ($\pi_T^\pm \rightarrow b\bar{c}, b\bar{u}$) process originates from the uncertainty on the b -tagging efficiencies, which is a 8.4% (9.4%) relative error for ST+ST, a 9.2% (17.0%) relative error for ST+JP, and a 4.3% (4.3%) relative error for ST+NNtag. Additional sources of systematic error include the jet energy scale, the lepton identification efficiency, parton distribution functions, and the initial and final state radiation models [22]. The systematic uncertainties associated with the shape of dijet invariant mass and Q -value are also studied by varying the jet energy scale and the initial and final state radiation, which are found to have a negligible impact on the final results.

Since there is no significant excess of events in the data compared to the predicted background, we set the 95% C.L. excluded region on technicolor production as a function of the technicolor particle mass. A 2-dimensional binned maximum-likelihood technique which assumes Poisson statistics is used on the 2-dimensional distribution of dijet invariant mass vs Q -value by constraining the number of background events within the uncertainties. To calculate the 95% C.L. excluded region, we use neutral and charged π_T signals simultaneously. A Bayesian interval is constructed from the cumulative likelihood distributions and a prior probability density function uniform in the number of technicolor signal events. The 95% confidence level upper limit is defined to be the value s_{up} for which $\int_0^{s_{\text{up}}} L(s)ds / \int_0^\infty L(s)ds = 0.95$. The number of signal events is then converted to a technicolor particle production cross section times branching fraction $\sigma(p\bar{p} \rightarrow W\pi_T^0(\pi_T^\pm)) \cdot BR(\pi_T^0(\pi_T^\pm) \rightarrow b\bar{b}(b\bar{c}, b\bar{u}))$.

The expected limits determined from pseudo experiments and the observed limits relative to the theoretical production rate are listed in Table II. The expected and observed 95% confidence level excluded region in the ρ_T - π_T mass plane is shown in Fig. 3. Almost the entire region we have looked at in this search is excluded at 95% confidence level, except the area near the $W\pi_T$ production threshold with $m(\rho_T) \geq 220 \text{ GeV}/c^2$ and $m(\pi_T) \geq 125 \text{ GeV}/c^2$.

In summary, we have performed a search for technicolor production $p\bar{p} \rightarrow \rho_T^{\pm/0} \rightarrow W^\pm \pi_T^{0/\mp} \rightarrow \ell\nu b\bar{b}$, $\ell\nu b\bar{c}$, or $\ell\nu b\bar{u}$ using 1.9 fb^{-1} of integrated luminosity accumulated by the CDF II detector. A large fraction of the region of $m(\rho_T) = 180 - 250 \text{ GeV}/c^2$ and $m(\pi_T) = 95 - 145 \text{ GeV}/c^2$ is excluded at 95% confidence level, based on the technicolor Straw Man model. This measurement excludes a much larger region than the previous Tevatron searches [6, 7].

We thank Ken Lane for many fruitful discussions, the Fermilab staff and the technical staffs of the participating institutions for their vital contributions. This work was supported

$m(\rho_T, \pi_T)$	Normalized Upper Limit		$m(\rho_T, \pi_T)$	Normalized Upper Limit	
GeV/ c^2	Observed Limit	Expected Limit	GeV/ c^2	Observed Limit	Expected Limit
(180,95)	0.30	$0.22^{+0.09}_{-0.11}$	(230,125)	0.60	$0.48^{+0.22}_{-0.18}$
(190,95)	0.27	$0.27^{+0.11}_{-0.13}$	(230,135)	0.72	$0.49^{+0.21}_{-0.19}$
(190,105)	0.44	$0.28^{+0.13}_{-0.13}$	(230,145)	1.61	$0.79^{+0.35}_{-0.29}$
(200,105)	0.37	$0.30^{+0.13}_{-0.13}$	(240,125)	0.71	$0.57^{+0.26}_{-0.20}$
(200,115)	0.59	$0.37^{+0.18}_{-0.14}$	(240,135)	0.65	$0.56^{+0.25}_{-0.21}$
(210,110)	0.36	$0.33^{+0.15}_{-0.15}$	(240,145)	0.86	$0.58^{+0.24}_{-0.24}$
(210,115)	0.42	$0.33^{+0.15}_{-0.13}$	(240,155)	1.94	$1.03^{+0.45}_{-0.37}$
(210,125)	0.88	$0.47^{+0.21}_{-0.17}$	(250,130)	0.75	$0.65^{+0.27}_{-0.25}$
(220,115)	0.59	$0.42^{+0.19}_{-0.17}$	(250,135)	0.76	$0.66^{+0.26}_{-0.26}$
(220,125)	0.52	$0.39^{+0.17}_{-0.15}$	(250,145)	0.69	$0.65^{+0.27}_{-0.25}$
(220,135)	1.22	$0.59^{+0.27}_{-0.23}$	(250,155)	1.02	$0.72^{+0.34}_{-0.26}$
(230,120)	0.67	$0.48^{+0.24}_{-0.18}$	(250,165)	2.01	$1.31^{+0.58}_{-0.44}$

TABLE II: Expected and observed upper limit on $\sigma(\rho_T \rightarrow \pi_T W^\pm) \times BR(\pi_T \rightarrow b\bar{q}) / (\sigma_{\text{theory}}(\rho_T \rightarrow \pi_T W^\pm) \times BR_{\text{theory}}(\pi_T \rightarrow b\bar{q}))$ as a function of the $m(\rho_T)$ and $m(\pi_T)$ hypothesis.

by the U.S. Department of Energy and National Science Foundation; the Italian Istituto Nazionale di Fisica Nucleare; the Ministry of Education, Culture, Sports, Science and Technology of Japan; the Natural Sciences and Engineering Research Council of Canada; the National Science Council of the Republic of China; the Swiss National Science Foundation; the A.P. Sloan Foundation; the Bundesministerium für Bildung und Forschung, Germany; the World Class University Program, the National Research Foundation of Korea; the Science and Technology Facilities Council and the Royal Society, UK; the Institut National de Physique Nucléaire et Physique des Particules/CNRS; the Russian Foundation for Basic Research; the Ministerio de Ciencia e Innovación, and Programa Consolider-Ingenio 2010, Spain; the Slovak R&D Agency; and the Academy of Finland.

[1] P. W. Higgs, Phys. Rev. Lett. **13**, 508 (1964).

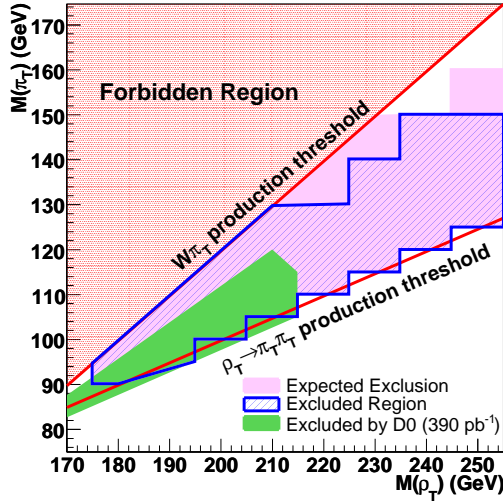


FIG. 3: 95% confidence level excluded region on technicolor particles production cross section times branching fraction as a function of $m(\rho_T)$ and $m(\pi_T)$ mass hypothesis. The expected excluded region from background-only pseudoexperiments are shown with the observed results from this analysis and D0 searches.

- [2] S. Weinberg, Phys. Rev. D **19**, 1277 (1979).
- [3] L. Susskind, Phys. Rev. D **20**, 2619 (1979).
- [4] C. T. Hill and E. H. Simmons, Phys. Rept. **381**, 235 (2003) .
- [5] K. D. Lane and S. Mrenna, Phys. Rev. D **67**, 115011 (2003) .
- [6] A. A. Affolder *et al.* (CDF collaboration), Phys. Rev. Lett. **84**, 1110 (2000).
- [7] V. M. Abazov *et al.* (D0 collaboration), Phys. Rev. Lett. **98**, 221801 (2007) .
- [8] T. Aaltonen *et al.* (CDF collaboration), Phys. Rev. D **80**, 012002 (2009) .
- [9] J. Abdallah *et al.* (DELPHI collaboration), Eur. Phys. J **22**, 17 (2001) .
- [10] T. Aaltonen *et al.* (CDF collaboration), Phys. Rev. D **71**, 052003 (2005) .
- [11] The CDF reference frame uses cylindrical coordinates, where z is the direction of the proton beam, and θ and ϕ are the polar and azimuthal angles with respect to the proton beam. The pseudorapidity is defined as $\eta = -\ln \tan \theta/2$, the transverse energy $E_T = E \sin \theta$, and the transverse momentum $p_T = p \sin \theta$. The missing transverse energy magnitude (\cancel{E}_T) is the vector sum of all calorimeter deposits, projected into the transverse plane. The \cancel{E}_T vector is corrected for the energy deposition of high- p_T muons as well as for jet energy corrections.

- [12] T. Aaltonen *et al.* (CDF collaboration), Phys. Rev. Lett. **100**, 041801 (2008).
- [13] A. Affolder *et al.* (CDF collaboration), Phys. Rev. D **64**, 032002 (2001).
- [14] M. L. Mangano, M. Moretti, F. Piccinini, R. Pittau, and A. D. Polosa, J. High Energy Phys. 07, 001 (2003).
- [15] T. Sjöstrand *et al.*, Comput. Phys. Commun. **135**, 238 (2001).
- [16] M. Cacciari, S. Frixione, G. Ridolfi, M. L. Mangano, and P. Nason, J. High Energy Phys. 04, 068 (2004).
- [17] F. Maltoni and T. Stelzer, J. High Energy Phys. 02, 027 (2003).
- [18] B. W. Harris, E. Laenen, L. Phaf, Z. Sullivan, and S. Weinzierl, Phys. Rev. D **66**, 054024 (2002).
- [19] D. Acosta *et al.* (CDF collaboration), Phys. Rev. D **71**, 052003 (2005).
- [20] J. M. Campbell and R. K. Ellis, Phys. Rev. D **60**, 113006 (1999).
- [21] A. Abulencia *et al.* (CDF collaboration), Phys. Rev. D **75**, 092004 (2007).
- [22] A. Bhatti *et al.* (CDF collaboration), Nucl. Instrum. Methods A **566**, 375 (2006).